Correct Diffusion Coefficients of Proteins in Fluorescence Correlation Spectroscopy. Application to Tubulin Oligomers Induced by Mg^{2+} and Paclitaxel

Tatiana Krouglova, Jo Vercammen, and Yves Engelborghs
Laboratory of Biomolecular Dynamics, Katholieke Universiteit Leuven, Celestijnenlaan 200D, B-3001 Leuven, Belgium

ABSTRACT   In view of recent warnings for artifacts in fluorescence correlation spectroscopy, the diffusion coefficient of a series of labeled proteins in a wide range of molecular mass (43–670 kD) was determined and shown to be correct with respect to published values and the theory. Fluorescence correlation spectroscopy was then applied to the study of fluorescently labeled tubulin and its oligomerization in vitro induced by Mg^{2+} ions, paclitaxel, and a fluorescent derivative of paclitaxel (Flutax2). By applying relations derived from the theory of Oosawa, we were able to determine the association constant of the oligomers induced by Mg^{2+}. With Flutax2 our experiments show that at nanomolar concentration, the fluorescent derivative is able to recruit tubulin dimers and to form oligomers of defined size. Flutax2 does not bind to microtubules preformed with paclitaxel, but it becomes preferentially incorporated into microtubules when Flutax2 oligomers are preformed, and microtubule formation is induced by paclitaxel addition. This shows that their incorporation into microtubules is faster than the displacement of the prebound drug. Experiments using fluorescently labeled tubulin and (unlabeled) paclitaxel confirm the induction of tubulin oligomers at limiting paclitaxel concentrations.

INTRODUCTION

In the context of the use of fluorescence correlation spectroscopy, recently a warning was published concerning the influence of a non-three-dimensional Gaussian shape of the confocal volume on the autocorrelation curve (Hess and Webb, 2002). It was shown that this could lead to the presence of a distorted curve that could be fitted with a second fast component when analyzed with the traditional equation for the autocorrelation curve. Moreover the slow component could be 80% off from the true diffusion coefficient. More recently an extensive documentation of other possible artifacts has been published (Enderlein et al., 2004). In this work we show that with the ConfoCor II instrument correct diffusion coefficients could be obtained for five different proteins in a wide range of molecular masses. In several cases, the labeled proteins show a fast component that was attributed to the presence of free dye, which was not removed even by a double chromatography step.

The technique was then applied to the study of tubulin and its oligomers. Microtubules are universal components of all eukaryotic cells, which play an important role in the building of the cytoskeleton, in cell division, and in intracellular transport. The basic structural subunit of microtubules is the protein tubulin. This tubulin molecule is a dimer of two 50-kD molecular mass polypeptide chains, designated α and β.

Different morphological structures of tubulin can be obtained by varying the solution conditions. In the presence of high concentration of Mg^{2+} tubulin can be assembled into microtubules and other polymeric forms like rings and spirals (Olmsted and Borisy, 1975; Frigon and Timasheff, 1975; Melki et al., 1989). Exchange of guanine nucleotide is strongly influenced by the presence of Mg^{2+} and therefore Mg^{2+} is required for the stability of tubulin (Croom et al., 1985; Correia et al., 1987). Tubulin binds also different drugs such as colchicine, vinblastine, podophyllotoxin, which inhibit tubulin assembly or depolymerize existing microtubules at micromolar concentrations.

Paclitaxel, originally isolated from the pacific yew *Taxus brevifolia* (Wani et al., 1971), inhibits cell division by strongly stabilizing microtubules. It enhances microtubule assembly by inhibition of the depolymerization of tubulin. Addition of paclitaxel can also lead to the formation of microtubule bundles in the cell (Schiff and Horwitz, 1980; Jordan et al., 1993). Nowadays, this drug is widely used in cancer chemotherapy and positive results have been reported in the treatment of several cancers (McGuire et al., 1989; Murphy, et al., 1993; Rowinsky et al., 1990).

In vitro, paclitaxel promotes the assembly of microtubules and stabilizes the structure by binding to the microtubule wall with a maximum stoichiometry of ~1 molecule/tubulin dimer (Parness and Horwitz, 1981; Díaz and Andreu, 1993). The mechanism of this microtubule stabilization is not fully clear. To understand this phenomenon, different approaches have been applied, for example the use of fluorescent derivatives of paclitaxel (Melan, 1998).

Investigations of the interaction of fluorescent analogs of paclitaxel with tubulin and microtubules have been carried out (Sengupta et al., 1995; Evangelio et al., 1998; Bicamumpaka and Page, 1998; Han et al., 1996). Several studies have shown that nonlabeled paclitaxel binds to microtubules in vitro, whereas high-affinity binding to

unpolymerized tubulin was not observed (Parness and Horwitz, 1981; Ringel and Horwitz, 1991; Díaz et al., 1993). Some studies, however, demonstrate that paclitaxel does interact with soluble tubulin in vitro, but with lower affinity ($K_d = 49 \pm 8$ μM at 25°C) (Sengupta et al., 1995) than that reported for polymeric tubulin, and it also binds to the tubulin-colchicine complex much more weakly than to microtubules (Howard and Timasheff, 1988; Carlier and Pantaloni, 1983).

In this article, fluorescent correlation spectroscopy (FCS) has been used to study the diffusion behavior of tubulin at concentrations down to the nanomolar range and in different conditions. In the presence of Mg^{2+} ions we observed a decreasing diffusion coefficient of fluorescently labeled tubulin, when increasing concentrations of unlabeled protein were added, and we were able to correlate this average diffusion coefficient with the degree of polymerization and to determine the association constant from its concentration dependence. We also studied the diffusion of the fluorescent derivative of paclitaxel ((7-O-[N-(2,7-difluoro-4′-fluoresceincarbonyl)-L-alanyl] paclitaxel (Flutax2) at nanomolar concentrations. The kinetic scheme and the reaction rates of Flutax2 binding to microtubules have already been determined by Díaz et al. (2000). These authors found that Flutax2 binds to microtubules with high affinity ($K \approx 10^7$ M^{-1} at 37°C), whereas the binding to tubulin under nonassembly conditions was not observed. Here we show that after addition of micromolar concentrations of tubulin, the diffusion coefficient of Flutax2 decreases due to the recruitment of multiple tubulin dimers and the formation of oligomers of defined size. Addition of extra paclitaxel to these oligomers does not displace the bound Flutax2 but induces microtubule formation with bound Flutax2.

Also paclitaxel (at limiting concentrations) is shown to induce tubulin oligomers made visible by using fluorescently labeled tubulin and extra tubulin.

MATERIALS AND METHODS

Preparation of tubulin

Microtubule proteins are isolated by two cycles of assembly/disassembly from pig brains according to the method of Shelanski et al. (1973) as modified by Engelborghs et al. (1977).

Microtubule protein concentration is estimated from the turbidity increase at 350 nm upon polymerization, using a specific turbidity change of 0.2 O.D./(mg/ml). Tubulin is purified from the microtubule proteins by phosphocellulose chromatography, and its concentration is determined spectrophotometrically in MES buffer using $\varepsilon_{278} = 120,000$ M^{-1} cm^{-1}.

The tubulin-colchicine complex is formed by incubation of tubulin with a millimolar solution of colchicine at room temperature for 30 min, followed by a separation from the free colchicine by chromatography on Sephadex G-25 (Sigma-Aldrich, St. Louis, MO). Dissociation of the complex is known to be very slow. The concentration of colchicine is determined spectrophotometrically using $\varepsilon_{350} = 16,600$ M^{-1} cm^{-1} (Wilson and Friedkin, 1966). The composition of the mixture was determined spectrophotometrically, and usually 0.9–1 mol colchicine/mol tubulin is found. The tubulin-podophyllotoxin complex is prepared by incubating the micromolar concentration of

tubulin with excess of podophyllotoxin (by a factor of 10) for 30 min at 25°C.

The MES buffer used is adjusted to pH 6.4 and has the following composition: 50 mM MES, 1 mM EGTA, 1 mM $MgCl_2$, and 1 mM NaN_3, with the ionic strength adjusted to 0.1 M with NaCl. Microtubules are assembled from purified tubulin in assembly MES buffer, containing 4 mM $MgCl_2$, 1 mM GTP, and paclitaxel at 37°C for 30 min. The addition of tubulin-colchicine complex to the assembly solution allows the production of short microtubules (Lambeir and Engelborghs, 1983).

Fluorescent paclitaxel derivative

Oregon Green 488 paclitaxel (Flutax2) is the fluorescent derivative of paclitaxel that is used to study interactions of fluorescent paclitaxel at nanomolar concentration with tubulin by FCS. Flutax2 (7-O-[N-(2,7-difluoro-4′-fluoresceincarbonyl)-L-alanyl] paclitaxel) was kindly provided by J. M. Andreu (CSIC, Madrid, Spain). It is synthesized by the reaction of 7-O-(L-alanyl) paclitaxel with Oregon Green 488 carboxylic acid, succinimidyl ester (''5 isomer'', ref. 0-6147, Molecular Probes, Eugene, OR) described before (Souto et al., 1995), and purified by preparative thin layer chromatography on silica gel with chloroform, methanol, and acetic acid 4:1:0.15 v/v/v as eluent. The mass spectrum and NMR data are in accordance with its structure (Souto, 1997). Flutax2 concentrations are measured in 0.5% sodium dodecyl sulfate, 50 mM sodium phosphate buffer pH 7.0 employing an extinction coefficient of $49,100 \pm 1100$ M^{-1} cm^{-1} at 496 nm (Díaz et al., 2000). Flutax2 is dissolved in dimethylsulfoxide at a final concentration of 1 mM and kept at −20°C.

For FCS measurements the fluorescent paclitaxel is diluted to the nanomolar range in MES buffer and added to the tubulin solution. Flutax2 has an excitation maximum that closely matches the 488-nm spectral line of the argon-ion laser.

Preparation of labeled tubulin

Labeled tubulin is obtained from microtubule proteins (MTP) that are labeled by an amine-reactive reagent such as carboxytetramethyl rhodamine succinimidyl ester (TAMRA) (C-1171, Molecular Probes) in the polymerized state at 37°C according to Hyman et al. (1991). The first step in the labeling procedure is the polymerization of microtubule proteins at concentrations of ~23 mg/ml at 37°C for 30 min followed by a change to the higher pH necessary for labeling. The microtubule solution is very carefully loaded onto a warm cushion containing Hepes buffer (pH 8.6), 60% (v/v) glycerol, and centrifuged at 30,000 rpm for 30 min at 37°C. The pellet is resuspended in warm Hepes buffer (pH 8.6) containing 40% (v/v) glycerol. TAMRA is added at a concentration of 100 μM to the microtubules and incubated at 37°C for 20 min while vortexing. To decrease the pH after labeling and stop the reaction, Pipes buffer (pH 6.8) containing 100 mM potassium glutamate and 40% (v/v) glycerol is added. This solution of microtubules is loaded on a warm cushion from Pipes buffer (pH 6.8) containing 60% glycerol and centrifuged at 30 rpm at 37°C for 30 min. The pellet of fluorescent microtubules is resuspended in Pipes buffer and depolymerized by incubation in an ice bucket for 20 min. This solution is then centrifuged at 4°C at 15,000 rpm for 30 min. To separate fluorescent tubulin from fluorescent microtubule associated proteins and from free dye, phosphocellulose chromatography and gel chromatography (PD10 column) are used, respectively. To check the activity of labeled tubulin an assembly control experiment was performed. The concentration of labeled tubulin is determined spectrophotometrically in MES buffer, using $\varepsilon_{278} = 120,000$ M^{-1} cm^{-1} for tubulin and $\varepsilon_{546} = 95,000$ M^{-1} cm^{-1} for TAMRA (Haugland, 2001). Labeling stoichiometries fall in the range of 0.4–0.7 mol TAMRA/ mol tubulin. In the FCS measurements the concentration of labeled tubulin is usually ~3 nM.

Preparation of labeled proteins

For FCS measurements different proteins with different molecular mass such as ovalbumin (43 kD), catalase (232 kDa), ferritin (440 kD), and thyroglobulin (669 kD) from the gel filtration calibration kit (17-0441-01, Amersham Biosciences, Piscataway, NJ) are labeled by TAMRA using the general procedure of labeling from Molecular Probes. TAMRA has an excitation maximum that closely matches the 543-nm spectral line of the He-Ne laser. Fluorescent bovine serum albumin (BSA) (65 kD), which is labeled by tetramethyl-rhodamine isothiocyanate, was obtained from Sigma (catalog no. A-2289).

Proteins are dissolved in 100 mM sodium borate buffer at pH 8.2 at room temperature, in concentrations varying from 50 μM to 100 μM. From a stock solution in DMSO, the amine-reactive probe is added drop-wise during a period of $\sim$1 min to the stirred protein solution, up to a final ratio of $\sim$10 mol of dye per mol of protein. To allow the reaction, the mixture of protein and dye is incubated at room temperature and stirred for 2 h. Freshly prepared hydroxylamine at 1.5 M, pH 8.5, is used to terminate the reaction and to remove weakly bound probes. Separation of the conjugate from unreacted dye is done by a double passage of the sample down a gel filtration column (PD10). The concentration of fluorescent proteins in the FCS measurements is in the nanomolar range.

Analytical ultracentrifugation

The sedimentation coefficient of tubulin, after phosphocellulose and gel chromatography, was determined using analytical boundary sedimentation in a Beckman optima XL-A analytical ultracentrifuge (Beckman, Fullerton, CA). At regular time intervals, absorption profiles were recorded at 280 nm, first at 20,000 rpm to sediment possible high molecular mass particles and then at 40,000 rpm to sediment tubulin dimers. All measurements were carried out at 23°C, and the data were processed as described elsewhere (Aerts et al., 1997).

Fluorescent correlation spectroscopy

FCS is applied to the analysis of oligomer formation of tubulin in the presence of Mg^{2+} and to the interaction of tubulin with Flutax2 using a commercial instrumental setup, i.e., the LSM 510-ConfoCor II (Zeiss, Oberkochen, Germany). This technique allows the determination of the diffusion characteristics of fluorescent molecules and their interaction with other particles at nanomolar concentrations in a femtoliter volume.

The principle of FCS is described by Rigler (Rigler and Mets, 1992; Rigler et al., 1993; Rigler and Widengren, 1990). The setup of the LSM 510-ConfoCor II is the following. Light from a laser is focused by the objective (40×, 1.2 N.A. Zeiss C-Apochromat, water immersion objective) into a solution of fluorescent molecules defining an excitation volume of $\sim$0.2 fl. For TAMRA-labeled tubulin the 543-nm line of a He-Ne laser is used. The measurements with fluorescent paclitaxel are performed using the argon-ion laser line at 488 nm. The fluorescence signal of the sample and the excitation laser light are separated by a main dichroic mirror (high transmission for emission light, high reflection for excitation light) in combination with a long-pass filter (LP-560), which is installed behind the objective. The emission light passes through a motor-controlled, variable pinhole (80 μm in diameter in all our experiments), which blocks the emission photons produced outside the laser waist, and is then focused onto an avalanche photodiode (APD). The photo current of the APD is passed into a correlator, which calculates the autocorrelation function of the fluorescence intensity fluctuations. The autocorrelation curve allows the determination of the particle number and the diffusion time.

Mathematically, a normalized correlation function $G(\tau)$ is defined as follows:

$$G(\tau) = \frac{\langle I(t) \rangle^2 + \langle \delta I(t) \delta I(t + \tau) \rangle}{\langle I(t) \rangle^2}, \tag{1}$$

where $\langle I(t) \rangle$ is the average fluorescence intensity, $\delta I(t)$ and $\delta I(t + \tau)$ are the deviations of the average fluorescence intensity at time t and $t + \tau$, respectively. τ is the timescale for the autocorrelation function.

The autocorrelation function is related to the diffusion time τ_d and excitation volume by the following relation (Rauer et al., 1996):

$$G(\tau) = 1 + \frac{1}{N} \left(\frac{1}{1 + \frac{\tau}{\tau_d}} \right)$$
$$\times \left(\frac{1}{1 + (\omega_1/\omega_2)^2 \tau/\tau_d} \right)^{1/2}$$
$$= 1 + \frac{1}{N} f(\tau/\tau_d), \tag{2}$$

where ω_1 and ω_2 are the radii of the Gaussian beam profile at $1/e^2$ of its maximal intensity in the radial and axial dimension of the laser beam, respectively. N is the average number of fluorescent molecules within the excitation volume.

The experimentally obtained autocorrelation function is analyzed with the ConfoCor II software package. To calibrate the ConfoCor and to determine the parameters ω_1 and ω_2, rhodamine 6G with a known diffusion coefficient $D = 2.8 \times 10^{-10}$ m^2/s at 20°C (Magde et al., 1974) is used. These parameters are then used to determine unknown diffusion coefficients and fractions of free and bound molecules. The relation between the diffusion coefficient D and the diffusion time τ_d can be obtained from the following equation:

$$\tau_d = \frac{\omega_1^2}{4D}. \tag{3}$$

In case of the binding of a fluorescent molecule to a target with a sufficiently smaller diffusion coefficient (a factor >2), the correlation function is now a sum of two fractions that diffuse independently:

$$G(\tau) = 1 + \frac{1}{N} [(1 - y) f(\tau/\tau_{free}) + \alpha^2 y f(\tau/\tau_{bound})] /$$
$$[(1 - y) + \alpha y]^2, \tag{4}$$

where $(1 - y)$ and y are the fraction of free and bound fluorescent ligands, respectively, τ_{free} and τ_{bound} are their respective diffusion times, and α is the ratio of the brightness of bound/free molecule (Rauer et al., 1996).

The laser power for the He-Ne and argon-ion lasers is set, respectively, to 1 mW and to 10 mW for all experiments. The actual power within the sample is much lower due to losses on lenses, beam splitter, and dichroic mirror. This power level is high enough to observe the fluorescence signal from each molecule and still low enough to keep photobleaching negligible. The significant advantages of the ConfoCor II are the small detection volume ($\sim$0.2 fl), the possibility to determine the ratio ω_2:ω_1 of the axes with very good accuracy (5.5 $\pm$ 1), and a diffraction-limited focal spot in the sample.

All FCS measurements were done in a sample volume of 100 μl. Concentrations of fluorescent molecules were in nanomolar range (between 3 and 15 nM) and concentrations of nonlabeled tubulin were varied in the micromolar range. The FCS measurements were done at room temperature (20°C) and in MES buffer. The measuring time per sample was 30 s and all samples were measured 10 times.

RESULTS

Labeled proteins in the FCS measurements

Recently, Hess and Webb (2002) have demonstrated that the observation volume in FCS under many measurement conditions could be non-Gaussian in three dimensions. This fact may lead to inaccurate results in the analysis of chemical kinetic processes, the apparent appearance of a second diffusing species, or some other type of nonstandard diffusion behavior. A signature of the non-Gaussian observation volume is a strong maximum in the count rate per molecule (cpm) as a function of the detector pinhole diameter (Hess and Webb, 2002).

We have checked for the presence of this signature in our measurements on the ConfoCor II by analyzing the dependence of the cpm as a function of the pinhole diameter. The results of this test are shown in Fig. 1. According to Hess and Webb (2002) a well-distinguished maximum must appear on the graph if the observation volume is not purely Gaussian. In our case the value increases and levels off as expected but the maximum opening is limited to 110 μm due to the limited size of the glass fiber used behind the pinhole and a further increase has no further influence.

Another signature of a non-Gaussian observation volume is the presence of a second component in the fitting of the autocorrelation function from the solution even containing only one type of molecules (Hess and Webb, 2002). In our instrument the correlation curves resulting from the measurements of the solution containing only dye molecules can be accurately fitted with a single component. Also in the case of the fluorescent protein ovalbumin the autocorrelation function can also be accurately fitted with a single component. The autocorrelation function and the residues are plotted in Fig. 2. The wavy shape of the plotted residuals

FIGURE 2   (A) Autocorrelation function of a solution containing labeled ovalbumin. The dashed line represents a one-component fit. The diffusion time of labeled ovalbumin (concentration 2 nM) is determined to be 166 μs. (B) Residuals for a one-component fit of the autocorrelation function.

indicative of a second component is not observed in this case.

Proteins with different molecular mass from gel filtration calibration kits such as ovalbumin (43 kD), catalase (232 kD), ferritin (440 kD), and thyroglobulin (669 kD) are labeled by TAMRA and characterized at nanomolar concentration in phosphate buffer (pH 7.0) by FCS. The absence of aggregates for all these nonlabeled proteins at this solution condition has been shown by sedimentation equilibrium under similar solution conditions in Beckman XLA analytical ultracentrifuge (Chacon et al., 2000).

In the fitting of the correlation curves of these labeled proteins the best fit is often obtained with a two-component model. The fast component is assumed to be due to the free dye, which seems to be difficult to remove, even after a double passage through a G25 column. To check if the fast component really corresponds to the free dye, the correlation function is fitted with a two-component model without fixing the diffusion time for the fast moving molecule. This fitting procedure has been done for all fluorescent proteins. The results show that the diffusion coefficient of the fast component remains practically invariant for the whole range of molecular masses (Fig. 3) and is equal to the diffusion coefficient of the fluorescent dye measured separately in buffer by FCS.

The second or slow component is attributed to the labeled protein. The dependence of the diffusion coefficient on the molecular mass of the different fluorescently labeled proteins is shown in Fig. 3.
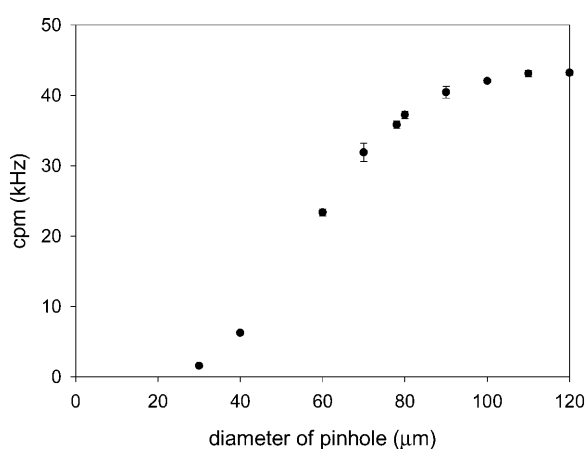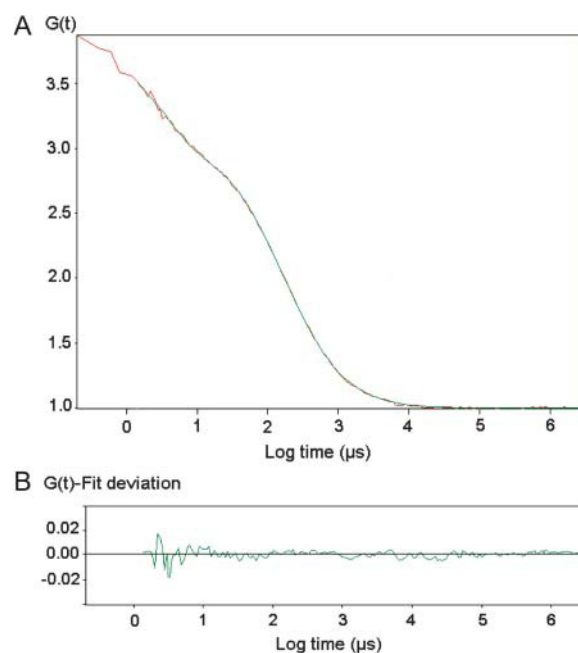

FIGURE 1   Dependence of the apparent count rate per molecule (cpm) on the diameter of the pinhole. The measurements are done on the LSM 510-ConfoCor II at nanomolar concentrations of rhodamine 6G. The absence of a pronounced maximum indicates a Gaussian distribution of the excitation light. In our instrument the maximal opening is limited to 110 μm due to the diameter of the glass fiber used between the pinhole and the APD.
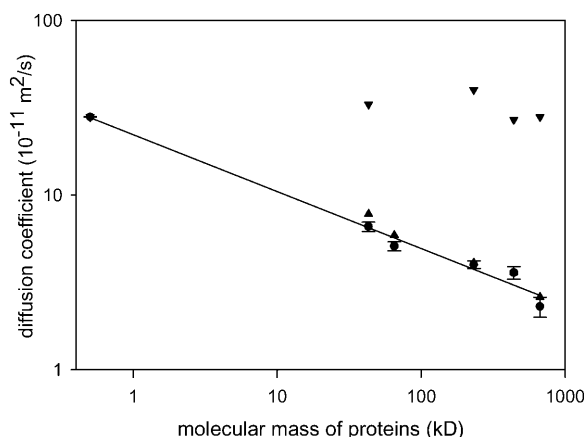
FIGURE 3 Dependence of the diffusion coefficient of labeled proteins on their molecular mass. Proteins ovalbumin (43 kD), catalase (232 kD), ferritin (440 kD), and thyroglobulin (669 kD) are labeled by TAMRA, except BSA (65 kD), which is labeled by tetramethyl-rhodamine isothiocyanate. All proteins are measured by FCS in phosphate buffer. Symbols (●) represent the experimental diffusion coefficients of the fluorescent proteins measured at nanomolar concentration by the ConfoCor II and (▲) are data from the literature. The data (▼) represent the diffusion coefficients of a small fraction of the free dye (TAMRA) present in the sample of labeled proteins.

The diffusion coefficient of the spherical particles can be calculated using the theoretical Stokes-Einstein relation:

$$D = \frac{kT}{6\pi\eta r}, \qquad (5)$$

where the Boltzmann constant $k = 1.38 \times 10^{-23}$ J/K, the absolute temperature $T = 293$ K, the viscosity of water $\eta = 10^{-3}$ kg/(ms), and r is the hydrodynamic radius of the molecule. The radius, r, can be calculated from the molecular mass of the molecule using the following formula:

$$r = \sqrt[3]{\frac{3m/N_A}{4\pi\rho}}, \qquad (6)$$

where N_A is Avogadro's number $= 6.023 \times 10^{23}$ mol^{-1}, and ρ is the mean density of the molecule, e.g., 1 g/ml. Theoretically, therefore, the diffusion coefficient D of the molecule is proportional to the molecular mass as $D \sim M^{-0.33}$. The experimental data are fitted by a linear regression (in log scale) and the proportionality coefficient (a) in our measurements for TAMRA-labeled proteins is determined to be $a = -0.32$, which is in very good agreement with the theoretical value. The diffusion coefficients obtained from the literature for all proteins from the gel calibration kit are also plotted in Fig. 3. As it can be seen, the diffusion coefficients of catalase, ferritin, and thyroglobulin measured by FCS, are similar to the diffusion coefficients measured by other techniques as obtained from the literature. The diffusion coefficients of ovalbumin and BSA in the FCS measurements are slightly lower than the

values found in the literature. After these studies we are confident that we can determine correct diffusion coefficients of proteins in a wide range of molecular mass values.

Labeled tubulin in the FCS measurements

The diffusion coefficient of fluorescently labeled tubulin is measured at nanomolar concentration in MES buffer. The best fit of the autocorrelation curve is again obtained by using a two-component model. Because the characteristic fast diffusion time corresponds to that of the free dye (TAMRA), its value is fixed at 39 ± 2 μs in further fittings. This value is obtained independently from FCS measurements on the free dye. The diffusion coefficient of fluorescently labeled tubulin at nanomolar concentration is found to be $(4.5 \pm 0.2) \times 10^{-11}$ m^2/s and remains the same when the concentration of labeled tubulin varies between 2 nM and 10 nM. The solution of fluorescent tubulin (even after a double passage down a gel column) still contains $\sim 20 \pm 4\%$ of free dye, as measured by FCS, which seems difficult to be removed. The stability of the labeled tubulin is checked by measuring the diffusion coefficient and the number of particles for at least 1 h. These values do not change during this time interval, which suggests that the labeled tubulin is stable and forms no aggregates during the time of an experimental session.

The interactions of labeled tubulin with unlabeled tubulin at different Mg^{2+} concentrations

The assembly of tubulin into microtubules and other polymeric forms, like rings and spirals is favored by high concentrations of Mg^{2+} as has been observed by velocity sedimentation by Frigon and Timasheff (1975). To find the diffusion coefficient of tubulin at micromolar concentration and at high Mg^{2+} the following experiment is done. Fluorescent tubulin at 3-nM concentration is added to different concentrations of nonlabeled tubulin varying from 0.2 μM up to 40 μM and the fluorescence fluctuations are observed. The autocorrelation function of this signal is analyzed and the diffusion coefficients are determined. The results are shown in Fig. 4. At 1 mM Mg^{2+} the mean value of the diffusion coefficient of the fluorescent tubulin in the presence of varying concentrations of unlabeled tubulin is determined to be $(4.3 \pm 0.1) \times 10^{-11}$ m^2/s. This value is similar to the value for labeled tubulin at nanomolar concentration in the same solution conditions and it is independent within uncertainty from the concentration of unlabeled tubulin. The concentrations of added labeled tubulin varied between 2 nM and 10 nM and this variation shows no influence on the obtained results.

At 16 mM of Mg^{2+} the diffusion coefficient of the species that we consider to be labeled tubulin decreases at increasing concentrations of unlabeled tubulin. We therefore consider it to be an average diffusion coefficient of a complex between
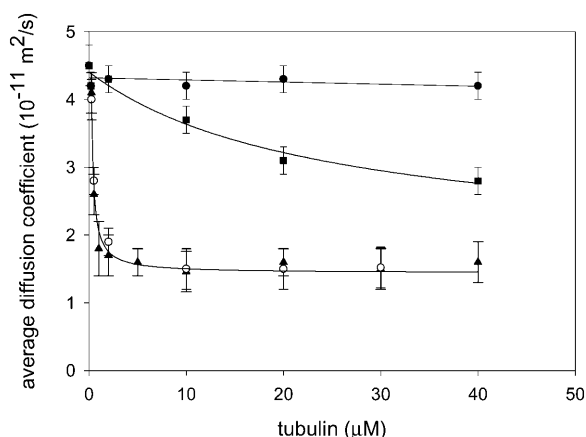
FIGURE 4 Formation of tubulin oligomers in the presence of 16 mM Mg^{2+} and paclitaxel. Measurements are carried out in 50 mM MES buffer, pH 6.4, 1 mM GDP. The diffusion coefficient of labeled tubulin (3 nM) is measured in the presence of increasing concentrations of unlabeled tubulin, respectively, in a 1-mM (●) and a 16-mM (■) concentration of Mg^{2+}. The plot (▲) and (○) represent the decreasing average diffusion coefficient of Flutax2-tubulin complex at 13-nM concentration of Flutax2 with increasing concentrations of unlabeled tubulin in MES buffer containing 1 mM Mg^{2+}, in the absence and in the presence of excess of podophyllotoxin, respectively.

labeled and unlabeled tubulin. At a concentration of 40 μM of unlabeled tubulin, the average diffusion coefficient is found to be $(2.8 \pm 0.2) \times 10^{-11}$ m^2/s. This value is much lower than the diffusion coefficient of the tubulin dimers at 1 mM Mg^{2+}. A continuous decrease of the diffusion coefficient as shown in Fig. 4, suggests that (at 16 mM of Mg^{2+}) tubulin oligomers of increasing size are being formed in the solution.

The oligomerization of the tubulin in the presence of high Mg^{2+} concentration has been described as being of the isodesmic type, followed by ring closure at higher tubulin concentrations (Frigon and Timasheff, 1975). At the concentrations of tubulin used here, ring closure does not yet occur and the open oligomer type prevails. This means that all steps in the polymerization are governed by the same association constant K. Such an open isodesmic polymerization process has been described by the theory of Oosawa and Kasai (1962). The theory predicts that in this type of polymerization the length of the oligomers is distributed exponentially.

To find the relationship between the average diffusion coefficient and the size of the tubulin oligomer, simulations were done using the computer program HYDROSUB developed by García de la Torre and Carrasco (2002). This program takes into account the hydrodynamic and other solution properties, as well as the spatial organization of the subunits, i.e., their mutual position and orientation. The subunits are modeled as simple shapes such as ellipsoids of revolution and cylinders. Owing to the axial symmetry of these shapes, a bead shell model is constructed for each subunit and a shell model of the whole particle is calculated.

The tubulin dimer can be modeled as a rigid structure composed of two identical compact ellipsoids (monomers) of

approximate dimensions $4.6 \times 4.0 \times 6.5$ nm (width, height, and depth, respectively) (Nogales et al., 1999). Two tubulin monomers bind to each other and form a tubulin dimer with dimensions $4.6 \times 8.0 \times 6.5$ nm (Nogales et al., 1999). To calculate the diffusion coefficient of the oligomers a complete specification of the structure of the whole assembly, with reference to a laboratory-fixed system of coordinates, requires, for each subunit: its dimensions, the three Cartesian coordinates of its center of mass, and the two sphericopolar angles, polar and longitudinal, that determine the orientation of the main symmetry axis. From these calculations the dependence of the diffusion coefficient on the size and the shape of the oligomer is obtained.

The average degree of oligomer formation $\langle i \rangle$ for small oligomers can be written as

$$\langle i \rangle = (D_0/D_i)^b, \qquad (7)$$

where D_0 and D_i are the diffusion coefficients (inversely proportional to the radius of the species) of tubulin dimer and tubulin oligomer (containing i dimers), respectively, and b is an exponent that is determined from the dependence of the simulated diffusion coefficient on the size and the shape of the oligomer.

Normally, the polymerization process involves two types of contacts between tubulin subunits: head-to-tail binding of dimers resulting in protofilaments that run along the length of the microtubule and lateral interactions between parallel protofilaments that complete the microtubule wall (Nogales et al., 1999). Using the HYDROSUB program, the parameter b was found to be 1.72 for the longitudinal type of contacts and 1.89 for the lateral associations.

According to the theory of Oosawa (Oosawa and Kasai, 1962) the following relation exists between the association constant and the mean length of oligomers:

$$Kc_1 = 1 - \frac{1}{\langle i \rangle}, \qquad (8)$$

where c_1 is the concentration of tubulin dimers and K is the association constant. The total concentration of tubulin C_{tot} according to Oosawa is:

$$C_{tot} = c_1 + \frac{c_1}{(1 - Kc_1)^2} = \left(\frac{1}{K}\right)\left(Kc_1 + \frac{Kc_1}{(1 - Kc_1)^2}\right)$$
$$= \frac{1}{K}f(Kc_1), \qquad (9)$$

where $f(Kc_1)$ is a shorthand for the full function of Kc_1. In this formulation a nucleation factor is assumed to be one.

Using Eq.9 the dependence of the function $f(Kc_1)$ on the total concentration of tubulin is plotted in Fig. 5 and the association constant K is determined to be 0.091 $\pm$ 0.004 μM^{-1} for a model with longitudinal and 0.108 $\pm$
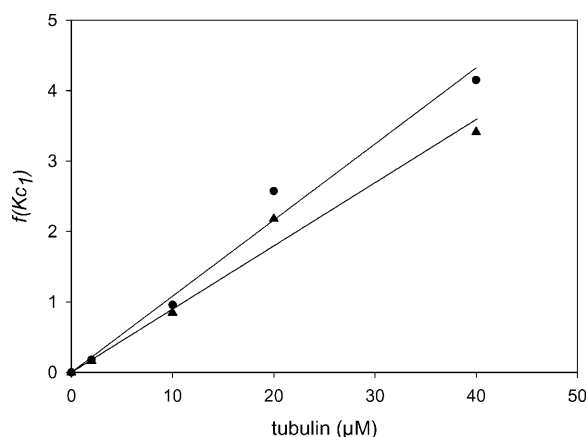
FIGURE 5 Binding plot for tubulin-tubulin interactions in the presence of 16 mM Mg^{2+}. Values of the function $f(Kc_1)$ for longitudinal (▲) and lateral contacts (●) calculated on the basis of the decreasing average diffusion coefficient (see text) as a function of tubulin concentration. The association constants are calculated from the slope and found to be equal to 0.091 ± 0.004 μM^{-1} and 0.108 ± 0.003 μM^{-1} for longitudinal (▲) and lateral contacts (●), respectively (at 20°C and in MES buffer with 1 mM GDP).
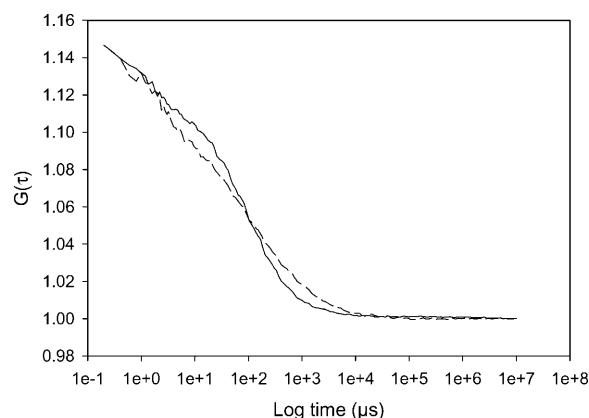

FIGURE 6 Autocorrelation functions of Flutax2 and a mixture of Flutax2 and tubulin. The solid line represents the autocorrelation function of a solution containing 13 nM of Flutax2. The diffusion time is determined to be 43 μs. This value is fixed in the fitting of the correlation curve for the mixture of Flutax2 and tubulin. The dashed line represents the autocorrelation function of a solution containing a mixture of Flutax2 and 10 μM tubulin. This autocorrelation function was fitted by a two-component model yielding 66% free Flutax2 and 34% bound Flutax2 to tubulin. The diffusion coefficient of the complex is determined to be (1.6 ± 0.3) 10^{-11} m^2/s.

0.003 μM^{-1} for a model with lateral associations (at room temperature and in MES buffer with 1 mM GDP). These values are in fair agreement with the results of Frigon and Timasheff (1975) and prove that the FCS method is able to analyze oligomer formation of tubulin and that the fluorescent labeling of tubulin does not interfere with the oligomerization process.

Pure Flutax2 in the FCS measurements

A fitting of a correlation curve resulting from the measurements of a solution containing only free Flutax2 gives a characteristic translational diffusion time $\tau = 43$ μs. This diffusion time of the free fluorescent derivative is then fixed in the fitting of the correlation curve for the mixture of fluorescent paclitaxel and tubulin. The diffusion coefficient of Flutax2 is determined to be $(2.2 \pm 0.2) \times 10^{-10}$ m^2/s. The autocorrelation curves of a solution containing free Flutax2 and a mixture of Flutax2 and tubulin (10 μM) are shown in Fig. 6.

Binding of Flutax2 to the tubulin

It is known that nonlabeled paclitaxel binds to microtubules in vitro with a maximum stoichiometry 1 mol of paclitaxel/mol of tubulin in microtubules and is supposed not to bind with high-affinity to unpolymerized tubulin (Parness and Horwitz, 1981; Ringel and Horwitz, 1991; Díaz et al., 1993). However, the fluorescent probe of paclitaxel such as Flutax2 that we use in this work binds to the free tubulin dimer at a concentration 0.25 μM of tubulin. In this experiment, Flutax2 at nanomolar concentration is added to different

concentrations of tubulin (in micromolar range) and the diffusion coefficient, the fractions of free and bound fluorescent paclitaxel are determined from the autocorrelation curves. The best-fitting result of the autocorrelation function is obtained with a two-component model with a fixed value for the diffusion time of Flutax2.

The diffusion coefficient of the tubulin-Flutax2 complex seems to be a function of the tubulin concentration as is shown in Fig. 4 and therefore is assumed to be an average diffusion coefficient of the complex itself and of an oligomeric species of the complex. The average diffusion coefficient of the tubulin-Flutax2 complex is calculated to be $(4.1 \pm 0.2) \times 10^{-11}$ m^2/s at a concentration of tubulin of 0.25 μM. At concentrations of tubulin varying between 0.5 μM and 10 μM the average diffusion coefficient of Flutax2 in complex with tubulin decreases with increasing tubulin concentration, but as seen in Fig. 4, at concentrations of tubulin >10 μM, the average diffusion coefficient remains the same at $\sim(1.6 \pm 0.3) \times 10^{-11}$ m^2/s. These changes in the average diffusion coefficient with increasing tubulin concentration suggest the recruitment of tubulin dimers by Flutax2 and at tubulin concentrations >10 μM, oligomers of defined size seem to be formed.

Fig. 7 demonstrates the interaction between Flutax2 and tubulin, i.e., it shows the dependence on the concentration of tubulin of the ratio of the amplitude fractions of tubulin-Flutax2 complex/free Flutax2. The amplitude fraction of the tubulin-Flutax2 complex is changed from 2% to 87% when the concentration of the tubulin is varied from 0.25 μM up to 50 μM. The measured amplitude fractions of both species at each concentration of tubulin do not change during the time span of the experiment.
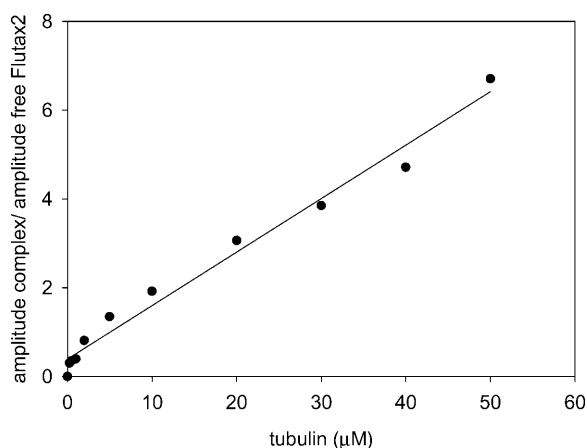
FIGURE 7 Interaction of Flutax2 and tubulin in MES buffer determined by FCS. Flutax2 at nanomolar concentration (13 nM) is added to different concentrations of tubulin (between 250 nM and 50 μM) in MES buffer. The ratio of bound/free Flutax2 is increasing with increasing tubulin concentration. The association constant can be obtained from the slope of the curve.

In our case, the experiments are done at low Mg^{2+} concentration and the added tubulin is always dimeric. The amount of the tubulin consumed in the oligomers induced by paclitaxel can be neglected compare to the total tubulin concentration. Therefore the free tubulin concentration can be assumed to be the total concentration and we can define the following equation

$$K_{ass}[Tu] = \frac{[Tu.FP]}{[FP]}, \tag{10}$$

where $[FP]$ is the concentration of free fluorescent paclitaxel, $[Tu]$ is the concentration of free tubulin and $[Tu.FP]$ is the concentration of fluorescent paclitaxel present in complex. The ratio of concentrations is equal to the ratio of amplitudes, when there is no fluorescence change upon binding.

However, when the fluorescent paclitaxel was added to tubulin, a reduction of the fluorescence signal per molecule was observed. This means that the fraction of paclitaxel in complex with tubulin, estimated from the amplitude fractions of the autocorrelation function, is underestimated, and the following equation for the calculating of the association constant has to be used (Van Craenenbroeck and Engelborghs, 1999):

$$K_{ass}[Tu] = \left(\frac{y}{1-y}\right)\frac{1}{\alpha^2}, \tag{11}$$

with

$$\alpha = \frac{(fpm)_{bound-Flutax2}}{(fpm)_{free-Flutax2}}, \tag{12}$$

where y and $1-y$ are amplitude fractions of bound and free fluorescent paclitaxel as measured by FCS, respectively, and α is the correction factor that can be determined when the fluorescence signal per molecule (*fpm*) for free and bound ligand is known.

In our case, the concentration of tubulin could not be increased enough to saturate fluorescent paclitaxel completely and thus the signal per molecule of bound fluorescent paclitaxel could not be determined directly. Therefore, an extrapolation of the fluorescence per particle to high tubulin concentrations was carried out, by fitting the fluorescence per particle to a saturation function (Van Craenenbroeck and Engelborghs, 1999):

$$fpm = \frac{fpm_0 + fpm_\infty K_{ass}[Tu]}{1 + K_{ass}[Tu]}, \tag{13}$$

where *fpm* is the average fluorescence signal per molecule and *fpm₀* and *fpm∞* are the fluorescence per molecule of free and bound Flutax2, respectively. The parameter fpm_∞ allowed the calculation of an α value of 0.41. (The same decrease in specific fluorescence was observed when Flutax2 was quantitatively bound to microtubules; see below). When this correction was considered in Eq. 11, K_{ass} was determined to be (0.12 ± 0.01) μM^{-1}. The association constant obtained from the fitting of the fluorescence per molecule (Eq. 13), was determined to be 0.14 μM^{-1}, which is in good agreement with the corrected association constant obtained from the fraction measurements (Eq. 11).

It should be noted that a small deviation from linearity occurs near the beginning of the binding plot (Fig. 7). We believe that this behavior of the plot can be explained by the heterogeneity of the system: added tubulin initially only binds to paclitaxel, and later also to the already formed tubulin-paclitaxel complex. (Another possibility that cannot be excluded is that the fluorescence decrease differs for the first and the subsequent tubulin molecules binding to Flutax2).

The interactions of Flutax2 with tubulin are also examined under nonassembly conditions: in MES buffer in the absence of Mg^{2+} ions and in the presence of podophyllotoxin (Schilstra et al., 1989). Podophyllotoxin is known as a drug that interacts with tubulin and prevents microtubule formation (Schilstra et al., 1989; Sackett, 1993). But in our measurements we found that the tubulin-podophyllotoxin complex can also form oligomers in the presence of nanomolar concentration of Flutax2. The diffusion coefficient of the tubulin-fluorescent paclitaxel complex is the same as for tubulin previously saturated with podophyllotoxin and then measured with fluorescent derivatives of paclitaxel by FCS (Fig. 4). No significant difference is found between tubulin and tubulin incubated with podophyllotoxin in the binding of Flutax2. Samples prepared with colchicine to make the tubulin-colchicine complex at different concentrations of the

complex also show no significant changes in the interaction of Flutax2 with tubulin. The diffusion coefficient of the tubulin-colchicine complex in the presence of Flutax2 decreases in the same way as for tubulin. The measurements are also done in a phosphate buffer and the same results are obtained.

Binding of paclitaxel to tubulin

Within a small concentration region we were able to show that paclitaxel itself can also induce oligomer formation of tubulin. The experiment was done at 4 nM of labeled tubulin in the presence of 3 μM of unlabeled tubulin and at 1 mM Mg^{2+}. As to be expected a value of $(4.1 \pm 0.2) \times 10^{-11}$ m^2/s was obtained for the diffusion coefficient. When 100 nM of paclitaxel was added to this tubulin solution the diffusion coefficient dropped to $(1.8 \pm 0.3) \times 10^{-11}$ m^2/s, showing the formation of oligomers.

Binding of Flutax2 to microtubules

The binding of Flutax2 to microtubules should be inhibited by an excess of paclitaxel, if Flutax2 and paclitaxel compete for the same binding site on microtubules. To prove this, a solution of 20 μM tubulin in MES buffer containing 4 mM MgCl$_2$, 1 mM GTP, and 40 μM paclitaxel is prepared and then incubated at 37°C for 30 min. Before FCS measurements, Flutax2 is added to this solution of microtubules. No binding of the Flutax2 is observed. The correlation curve stays the same as for free Flutax2.

Flutax2 at nanomolar concentration also forms tubulin oligomers in the presence of colchicine and these oligomers have the same diffusion coefficient as in the absence of colchicine. When 20 μM tubulin in MES buffer, containing 1 mM MgCl$_2$, 1 mM GTP, and 13 μM tubulin-colchicine complex (to produce short microtubules later on; Lambeir and Engelborghs, 1983) is incubated at 37°C for 30 min with Flutax2 at nanomolar concentration and an FCS measurement is done, the analysis of the autocorrelation curves with the two-component model gives the same diffusion coefficient for the complex of $(1.6 \pm 0.3) \times 10^{-11}$ m^2/s. The addition of saturating amounts of paclitaxel to this solution induces the assembly of tubulin into microtubules with the incorporation of Flutax2. This can be seen from the changes in the average diffusion coefficient of the complex during 20 min and this corresponds to the formation of microtubules (Fig. 8). It should be noted that the presence of the tubulin-colchicine complex guarantees the formation of a rather narrow distribution of short microtubules (Lambeir and Engelborghs, 1983). The average diffusion coefficient for microtubules after 20 min was determined to be 4.1×10^{-12} m^2/s. Atomic force microscopy measurements (not shown) of this sample containing short microtubules were performed and the average length of microtubules was measured to be 423 ± 93 nm. The theoretical diffusion coefficient of these microtubules was calculated by using the formula for the
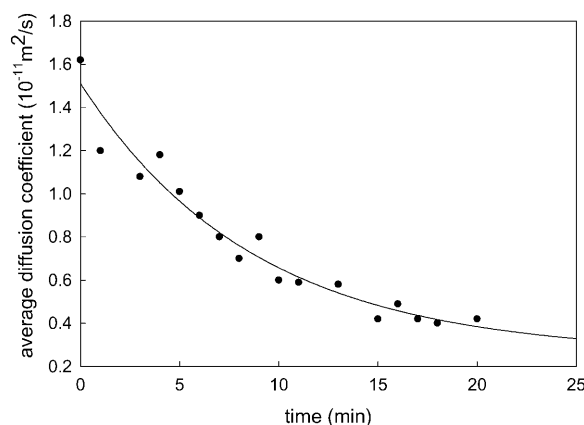

FIGURE 8 Assembly of tubulin into short microtubules in the presence of paclitaxel. Flutax2 at nanomolar concentration was added to tubulin (20 μM) and tubulin-colchicine complex at 13 μM and incubated at 37°C for 30 min in MES buffer, 1 mM GTP, and 1 mM Mg^{2+}. For the FCS measurements paclitaxel at 20-μM concentration was added to the solution of tubulin, Flutax2, and tubulin-colchicine.

translational diffusion coefficient of rod molecules (Tirado et al., 1984):

$$D = \frac{AkT}{3\pi\eta L},$$ (14)

where A is a correction factor:

$$A = \ln\left(\frac{L}{d}\right) + 0.312 + \frac{0.565}{L/d} - \frac{0.1}{(L/d)^2}.$$ (15)

L is the length of the molecule, d is the diameter of the rod molecule (for microtubules $d = 25$ nm), and the other parameters are as defined before. These calculations give the value of the average diffusion coefficient for this length of microtubules of 3.2×10^{-12} m^2/s, which is in fair agreement with data from FCS measurements.

Analytical ultracentrifugation

To be sure that the tubulin after purification by phosphocellulose and gel chromatography is present in its dimeric state, a boundary sedimentation experiment is done. Two tubulin concentrations are measured in the same buffer conditions as in the FCS experiments only with lowered GDP concentration (50 μM instead of 1 mM), which minimized the background absorption at 280 nm. The tubulin concentrations in those experiments are 5 μM and 10 μM. Analysis shows that 90–95% of the tubulin molecules have a sedimentation coefficient of 6.5 S. This value is close to the reported value for tubulin dimer (Detrich and Williams, 1978).

DISCUSSION

In this article we wanted to determine absolute diffusion coefficients and we first showed that we are able to do this for a wide variety of molecular masses. We also show that our instrument does not suffer from non-Gaussian excitation profiles.

The nice correlation between the diffusion coefficients and the molecular mass of several proteins (ovalbumin, BSA, catalase, ferritin, thyroglobulin) obtained from FCS measurements, corresponds perfectly with theory. This correlation allows us to estimate the molecular mass of tubulin in different conditions.

The analysis of tubulin oligomerization in the presence of magnesium ions has also been described in this article. High magnesium concentrations induce the formation of tubulin oligomers and rings. In our experiments we found that at a concentration of 16 mM of $MgCl_2$ the diffusion coefficient decreases with increasing tubulin concentration and this reflects the formation of open oligomers. The value of the diffusion coefficient of tubulin at its highest concentration obtained, in the presence of 16 mM Mg^{2+}, is determined to be $(2.8 \pm 0.3) \times 10^{-11}$ m^2/s. We suppose that this diffusion coefficient is for oligomers of the tubulin dimer and we estimate it would contain not more than six tubulin dimers, as the diffusion coefficient of thyroglobulin with molecular mass of 669 kD is equal to 2.4×10^{-11} m^2/s. The diffusion coefficient we obtain is still higher than the value of 2.2×10^{-11} m^2/s of the cryptophycin-tubulin rings (containing eight dimers) also measured with FCS (Boukari et al., 2003).

Applying the theory of Oosawa and Kasai (1962) to the formation of tubulin oligomers allows us to obtain the association constant in the presence of 16 mM Mg^{2+}. This value is determined to be 0.091 ± 0.004 μM^{-1} for the longitudinal model and 0.108 ± 0.003 μM^{-1} for the lateral model. Both values are in good agreement with the data obtained by Frigon and Timasheff (1975) and we cannot make the distinction between the two shapes.

The forms of the tubulin oligomers that are studied in this article are different from tubulin rings. This can be concluded from the values of the diffusion coefficients of tubulin oligomers determined by FCS in the presence of Mg^{2+} and Flutax2. These values are still higher than the values for tubulin rings 4.9×10^{-12} m^2/s (Palmer et al., 1982) measured by a quasielastic laser light scattering.

The expected diffusion constant of the tubulin dimer is estimated from the Svedberg equation (Gethner et al., 1977) to be 4.7×10^{-11} m^2/s. Using laser light scattering a diffusion coefficient of 4.41×10^{-11} m^2/s is found, which is very close. The diffusion coefficient of fluorescent BSA with molecular mass of 65 kD is determined to be $(5.1 \pm 0.3) \times 10^{-11}$ m^2/s. Therefore, in our investigations the highest value of the diffusion coefficient of tubulin can be attributed to dimeric tubulin with molecular mass of 100 kD, showing that tubulin is not dissociated into monomers at nanomolar concentrations. These results are in agreement with the finding by Caplow and Fee (2002) of a dissociation constant of 10^{-11} M for tubulin dimers determined by surface plasmon resonance.

All measurements with tubulin are done after cold centrifugation at 4°C for 20 min to remove aggregates of tubulin. The analytical ultracentrifugation is also done to prove that no oligomers are previously present in the preparation of tubulin. The labeled tubulin is also measured at its concentrations varying between 2 nM and 10 nM and in the presence of nonlabeled tubulin. No significant differences are obtained in the diffusion coefficient and this proves the absence of tendency of labeled tubulin to aggregate at low Mg^{2+} and nonassembly conditions.

We also studied the diffusion of fluorescent paclitaxel. The main conclusion of this work is that a nanomolar concentration of fluorescent paclitaxel is able to recruit tubulin dimers, leading to the formation of tubulin oligomers with a finite size.

Fluorescent derivatives of paclitaxel have already been studied by several authors. Some of them preferentially bind to microtubules, others to the unpolymerized, dimeric form. In our investigations we found evidence for the interaction of Flutax2 with tubulin in the dimeric state, already at tubulin concentrations of 0.25 μM. The diffusion coefficient of this complex is determined to be $(4.1 \pm 0.3) \times 10^{-11}$ m^2/s. With increasing concentration of tubulin the diffusion coefficient decreases down to $(1.6 \pm 0.3) \times 10^{-11}$ m^2/s indicating the formation of tubulin oligomers around the Flutax2 molecules.

We found no binding of Flutax2 to microtubules preformed in the presence of excess paclitaxel, showing that the Flutax2 binding site is not available on paclitaxel-saturated microtubules. But FCS measurements show the incorporation of Flutax2 in microtubules, when tubulin-Flutax2 oligomers are preformed and microtubules are induced by addition of paclitaxel (close to stoichiometric amounts). These results suggest that preformed tubulin-Flutax2 oligomers are incorporated into microtubules and might be preferential nucleation sites.

A sharp decrease of the average diffusion coefficient of the tubulin-Flutax2 complex upon addition of micromolar concentrations of tubulin (Fig. 4) and the deviation from linearity near the beginning of the binding plot (Fig. 7) probably indicate that tubulin has a high affinity for Flutax2 and that the binding of further tubulin molecules to this complex decreases in affinity upon increasing the size of the oligomers. This type of assembly of tubulin oligomers induced by nanomolar concentration of Flutax2 is different from the open assembly that occurs in the presence of high concentration of Mg^{2+}. This behavior is suggestive of a mechanism of cumulative strain, where successive association steps occur with decreasing affinity, a process that is formally similar to what happens in myosin self-assembly (Davis, 1981) and that explains the finite size of the oligomers.

Using FCS, an average equilibrium dissociation constant is determined to be (8.3 ± 0.7) μM for binding of tubulin to Flutax2 at nanomolar concentration. This value is similar to the data of Carlier and Pantaloni (1983) (equilibrium dissociation constant of 13 μM), but they measured the binding of paclitaxel to tubulin-colchicine complex in the dimeric form from the increase in GTPase activity of the tubulin-colchicine complex accompanying paclitaxel binding. Sengupta et al. (1995) measured the binding of *N*-debenzoyl-*N*-[3-(dimethylamino)benzoyl]-paclitaxel, another fluorescent derivative of paclitaxel, to dimeric tubulin and determined an equilibrium dissociation constant of 49 μM for binding of paclitaxel to unpolymerized tubulin, a value that is much higher than for Flutax2.

Our experiments with paclitaxel also demonstrate that the unlabeled molecule is able to induce oligomer formation. These oligomers can be end products when paclitaxel concentration is limiting, or intermediates of microtubule formation in excess concentrations of paclitaxel.

It is known that polymers composed of pure tubulin disassemble in the presence of podophyllotoxin (Schilstra et al., 1989). However, in this study we found that tubulin oligomers also can be formed when tubulin is first saturated with podophyllotoxin or colchicine and then the fluorescent paclitaxel is added. No significant difference in binding of Flutax2 is found between tubulin and tubulin incubated with podophyllotoxin. The values of the diffusion coefficients of the tubulin-Flutax2 complex in the presence of colchicine or podophyllotoxin remain the same as in the absence of these drugs.

REFERENCES

Aerts, T., J. Clauwaert, P. Haezebrouck, E. Peeters, and H. Van Dael. 1997. Interaction of detergents with bovine lens alpha-crystallin: evidence for an oligomeric structure based on amphiphilic interactions. *Eur. Biophys. J.* 25:445–454.

Bicamumpaka, C., and M. Page. 1998. *In situ* localization of paclitaxel binding structures: labeling with a paclitaxel fluorescent analogue. *Int. J. Mol. Med.* 2:161–165.

Boukari, H., R. Nossal, and D. L. Sackett. 2003. Stability of drug-induced tubulin rings by fluorescence correlation spectroscopy. *Biochemistry.* 42:1292–1300.

Caplow, M., and L. Fee. 2002. Dissociation of the tubulin dimer is extremely slow, thermodynamically very unfavorable, and reversible in the absence of an energy source. *Mol. Biol. Cell.* 13:2120–2131.

Carlier, M.-F., and D. Pantaloni. 1983. Taxol effect on tubulin polymerization and associated guanosine 5'-triphosphate hydrolysis. *Biochemistry.* 22:4814–4822.

Chacon, P., F. J. Diaz, F. Moran, and J. M. Andreu. 2000. Reconstruction of protein form with X-ray solution scattering and a genetic algorithm. *J. Mol. Biol.* 299:1289–1302.

Correia, J. J., L. T. Baty, and R. C. Williams, Jr. 1987. Mg^{2+} dependence of guanine nucleotide binding to tubulin. *J. Biol. Chem.* 262:17278–17284.

Croom, H. B., J. J. Correia, L. T. Baty, and R. C. Williams, Jr. 1985. Release of exchangeably bound guanine nucleotide from tubulin in a magnesium-free buffer. *Biochemistry.* 24:768–775.

Davis, J. S. 1981. Pressure-jump studies on the length-regulation kinetics of the self-assembly of myosin from vertebrate skeletal muscle into thick filament. *Biochem. J.* 197:309–314.

Detrich, H. W., and R. C. Williams. 1978. Reversible dissociation of the $\alpha\beta$ dimer of tubulin from bovine brain. *Biochemistry.* 17:3900–3907.

Díaz, J. F., and J. M. Andreu. 1993. Assembly of purified GDP-tubulin into microtubules induced by taxol and taxotere: reversibility, ligand stoichiometry, and competition. *Biochemistry.* 32:2747–2755.

Díaz, J. F., M. Menendez, and J. M. Andreu. 1993. Thermodynamics of ligand-induced assembly of tubulin. *Biochemistry.* 32:10067–10077.

Díaz, J. F., R. Strobe, Y. Engelborghs, A. A. Souto, and J. M. Andreu. 2000. Molecular recognition of taxol by microtubules. *J. Biol. Chem.* 275:26265–26276.

Enderlein, J., I. Gregor, D. Patra, and J. Fitter. 2004. Art and artefacts of fluorescence correlation spectroscopy. *Curr. Pharm. Biotechnol.* 5:155–161.

Engelborghs, Y., L. De Maeyer, and N. Overbergh. 1977. A kinetic analysis of microtubules *in vitro*. *FEBS Lett.* 80:81–85.

Evangelio, J. A., M. Abal, I. Barasoain, A. A. Souto, M. P. Lillo, A. U. Acuña, F. Amat-Guerri, and J. M. Andreu. 1998. Fluorescent taxoids as probes of the microtubule cytoskeleton. *Cell Motil. and Cytoskel.* 39:73–90

Frigon, R. P., and S. N. Timasheff. 1975. Magnesium-induced self-association of calf brain tubulin. I. Stoichiometry. *Biochemistry.* 14:4559–4566.

García de la Torre, J., and B. Carrasco. 2002. Hydrodynamic properties of rigid macromolecules composed of ellipsoidal and cylindrical subunits. *Biopolymers* 63:163–167

Gethner, J. S., G. W. Flynn, B. J. Berne, and F. Gaskin. 1977. Equilibrium components of tubulin preparations. *Biochemistry.* 16:5781–5785.

Han, Y., A. G. Chaudhary, M. D. Chordia, D. L. Sackett, B. Perez-Ramirez, D. G. I. Kingston, and S. Bane. 1996. Interaction of a fluorescent derivative of paclitaxel(Taxol) with microtubules and tubulin-colchicine. *Biochemistry.* 35:14173–14183.

Haugland, R. P. 2001. Handbook of Fluorescent Probes and Research Chemicals, 9th ed. J. Gregory, editor. Molecular Probes, Eugene, OR.

Hess, S. T., and W. W. Webb. 2002. Focal volume optics and experimental artifacts in confocal fluorescence correlation spectroscopy. *Biophys. J.* 83:2300–2317.

Howard, W. D., and S. N. Timasheff. 1988. Linkages between the effects of taxol, colchicine, and GTP on tubulin polymerization. *J. Biol. Chem.* 263:1342–1346.

Hyman, A., D. Drechsel, D. Kellogg, S. Salser, K. Sawin, P. Steffen, L. Wordeman, and T. Mitchison. 1991. Preparation of modified tubulins. *Methods Enzymol.* 196:478–480.

Jordan, M. A., R. J. Toso, D. Thrower, and L. Wilson. 1993. Mechanism of mitotic block and inhibition of cell proliferation by taxol at low concentrations. *Proc. Natl. Acad. Sci. USA.* 90:9552–9556.

Lambeir, A., and Y. Engelborghs. 1983. A quantitative description of microtubule formation in the presence of tubulin-colchicine. *Eur. J. Biochem.* 132:369–373.

Magde, D., E. L. Elson, and W. Webb. 1974. Fluorescence correlation spectroscopy. II. An experimental realization. *Biopolymers.* 13:29–61.

McGuire, W. P., E. K. Rowinsky, N. B. Rosensheim, F. C. Grumbine, D. S. Ettinger, and D. K. Armstrong. 1989. Taxol: a unique antineoplastic agent with significant activity in advanced ovarian epithelial neoplasms. *Ann. Intern. Med.* 111:273–279.

Melan, M. A. 1998. Use of fluorochrome-tagged taxol to produce fluorescent microtubules in solution. *Biotechniques*. 25:188–192.

Melki, R., M.-F. Carlier, D. Pantaloni, and S. N. Timasheff. 1989. Cold depolymerization of microtubules to double rings: geometric stabilization of assemblies. *Biochemistry*. 28:9143–9152.

Murphy, W. K., F. V. Fossella, R. J. Winn, D. M. Shin, H. E. Hynes, H. M. Gross, E. Davilla, J. Leimert, H. Dhingra, and M. N. Raber. 1993. Phase II study of taxol in patients with untreated advanced non small cell lung cancer. *J. Natl. Cancer Inst*. 85:384–388.

Nogales, E., M. Whittaker, R. A. Milligan, and K. H. Downing. 1999. High-resolution model of the microtubule. *Cell*. 96:79–88.

Olmsted, J. B., and G. G. Borisy. 1975. Ionic and nucleotide requirements for microtubule polymerization in vitro. *Biochemistry*. 14:2996–3005.

Oosawa, F., and M. Kasai. 1962. A theory of linear and helical aggregations of macromolecules. *J. Mol. Biol*. 4:10–21.

Palmer, G. R., D. C. Clark, P. M. Bayley, and D. B. Sattelle. 1982. A quasi-elastic laser light scattering study of tubulin and microtubule protein from bovine brain. *J. Mol. Biol*. 160:641–658.

Parness, J., and S. B. Horwitz. 1981. Taxol binds to polymerized tubulin *in vitro*. *J. Cell Biol*. 91:479–487.

Rauer, B., E. Neumann, J. Widengren, and R. Rigler. 1996. Fluorescence correlation spectrometry of the interaction kinetics of tetramethylrhodamin alpha-bungarotoxin with *Torpedo californica* acetylcholine receptor. *Biophys. Chem*. 58:3–12.

Rigler, R., and Ü. Mets. 1992. Diffusion of single molecules through a Gaussian laser beam. *SPIE Proc*. 1921:239–248.

Rigler, R., Ü. Mets, J. Widengren, and P. Kask. 1993. Fluorescence correlation spectroscopy with high count rate and low background: Analysis of translational diffusion. *Eur. Biophys. J*. 22:169–175.

Rigler, R., and J. Widengren. 1990. Ultrasensitive detection of single molecules by fluorescence correlation spectroscopy. *Bioscience*. 3:180–183.

Ringel, I., and S. B. Horwitz. 1991. Effect of alkaline pH on taxol-microtubule interactions. *J. Pharmacol. Exp. Ther*. 259:855–860.

Rowinsky, E. K., L. A. Cazenave, and R. C. Donehower. 1990. Taxol: a novel investigational antimicrotubule agent. *J. Natl. Cancer Inst*. 82:1247–1259.

Sackett, D. L. 1993. Podophyllotoxin, steganacin and combretastatin: natural products that bind at the colchicine site of tubulin. *Pharmac. Ther*. 59:163–228.

Schiff, P. B., and S. B. Horwitz. 1980. Taxol stabilizes microtubules in mouse fibroblast cells. *Proc. Natl. Acad. Sci. USA*. 77:1561–1565.

Schilstra, M. J., S. R. Martin, and P. M. Bayley. 1989. The effect of podophyllotoxin on microtubule dynamics. *J. Biol. Chem*. 264:8827–8834.

Sengupta, S., T. C. Boge, G. I. Georg, and R. H. Himes. 1995. Interaction of a fluorescent paclitaxel analogue with tubulin. *Biochemstry*. 34:11889–11894.

Shelanski, M. L., F. Gaskin, and C. R. Cantor. 1973. Microtubule assembly in the absence of added nucleotides. *Proc. Natl. Acad. Sci. USA*. 70:765–768.

Souto, A. A. 1997. Sintesis, caracterizacion, y aplicaciones de nuevas soudas fluorescents, para membranes y proteinas. Acidos peutaenoicos conjugados y derivados de taxol. PhD thesis. Universidad Complutense de Madrid, Madrid, Spain.

Souto, A. A., A. U. Acuña, J. M. Andreu, I. Barasoain, M. Abal, and F. Amat-Guerri. 1995. New fluorescent water-soluble taxol derivatives. *Angew. Chem. Int. Ed. Eng*. 34:2710–2712

Tirado, M., Lopez Martinez, C., and Garcia de la Torre, J.1984. Comparison of theories for the translational and rotational diffusion coefficients of rod-like macromolecules. Application to short DNA fragments. *J. Chem. Phys*. 81:2045–2052

Van Craenenbroeck, E., and Y. Engelborghs. 1999. Quantitative characterization of the binding of fluorescently labeled colchicine to tubulin in vitro using fluorescence correlation spectroscopy. *Biochemistry*. 38:5082–5088.

Wani, M. C., H. L. Taylor, M. E. Wall, P. Coggon, and A. T. McPhail. 1971. Plant antitumor agents. VI. The isolation and structure of taxol, a novel antileukemic and antitumor agent from *Taxus brevifolia*. *J. Am. Chem. Soc*. 93:2325–2327.

Wilson, L., and M. Friedkin. 1966. The biochemical events of mitosis. *Biochemistry*. 5:2463–2468.